RESEARCH REPORTS
Biomaterials & Bioengineering

B.R. Lawn[1*], Y. Deng[2], I.K. Lloyd[2], M.N. Janal[3], E.D. Rekow[3], and V.P. Thompson[3]

[1]Materials Science and Engineering Laboratory, National Institute of Standards and Technology, Gaithersburg, MD 20899-8500; [2]Department of Materials and Nuclear Engineering, University of Maryland, College Park, MD 20742-2115; and [3]University of Medicine and Dentistry of New Jersey, Dental School, 110 Bergen Street, Newark, NJ 07103-2400; *corresponding author, brian.lawn@nist.gov

J Dent Res 81(6):433-438, 2002

Materials Design of Ceramic-based Layer Structures for Crowns

ABSTRACT

Radial cracking has been identified as the primary mode of failure in all-ceramic crowns. This study investigates the hypothesis that critical loads for radial cracking in crown-like layers vary explicitly as the square of ceramic layer thickness. Experimental data from tests with spherical indenters on model flat laminates of selected dental ceramics bonded to clear polycarbonate bases (simulating crown/dentin structures) are presented. Damage initiation events are video-recorded *in situ* during applied loading, and critical loads are measured. The results demonstrate an increase in the resistance to radial cracking for zirconia relative to alumina and for alumina relative to porcelain. The study provides simple *a priori* predictions of failure in prospective ceramic/substrate bilayers and ranks ceramic materials for best clinical performance.

KEY WORDS: dental ceramics, elastic modulus, hardness, fracture, layer structures, material design, strength, toughness.

Received December 12, 2000; Last revision February 20, 2002; Accepted April 4, 2002

INTRODUCTION

Background

Ceramics are attractive materials for use in dental crowns because of their aesthetics, inertness, and biocompatibility. But all ceramics are brittle, to a greater or lesser extent, and tend to fail beyond a critical load or lifetime (Lawn, 1993). Even all-ceramic crowns fabricated with aesthetic but weak veneer porcelains on strong support alumina cores (InCeram) are subject to premature failure (Kelly, 1999). In the clinical context, we need to understand the fundamental mechanics of failure in dental ceramics on soft dentin-like underlayers under conditions that simulate basic occlusal function, so that a proper foundation can be laid for rational materials design of future multilayer crown structures.

The basic elements of occlusal function can be simulated in the laboratory by controlled contact testing (DeLong and Douglas, 1983). In the last decade, tests on monolithic polycrystalline ceramics (Guiberteau *et al.,* 1993; Lawn, 1998; Peterson *et al.,* 1998a; Rhee *et al.,* 2001a) indicate two modes of damage in the near-contact field: brittle mode—in small-grain, high-strength ceramics, with classic cone-like tensile cracks initiating from the upper surface; and *quasi*-plastic mode—in coarse-grain, high-toughness ceramics, with distributed shear-microcracks initiating within a subsurface "yield" zone. Analogous contact tests on flat ceramic layers joined to dentin-like soft substrates (Wuttiphan *et al.,* 1996; Chai *et al.,* 1999; Jung *et al:,* 1999; Chai and Lawn, 2000) indicate a third mode, radial cracking at the inner surface (*i.e.*, at the ceramic-layer/substrate interface), driven by undersurface tension from flexure of the ceramic layer on the soft support substrate. This last mode is considered most relevant in the context of failure of all-ceramic crowns, because it can occur at relatively low loads and spread over long lateral distances. Moreover, it may remain entirely subsurface, and therefore pass undetected in opaque materials.

Independent studies in the clinical literature on simulated crown structures, mostly flat-layer ceramics on composite resin bases in various forms of upper-surface contact loading, acknowledge the existence of at least two of the above damage modes (Scherrer and Rijk, 1993; Scherrer *et al.*, 1994; Kelly, 1997; Tsai *et al.,* 1998)—specifically, outer-surface Hertzian-like cracks and inner-surface radial cracks, depending on loading and layer geometry. Kelly and others (Kelly *et al.,* 1990; Thompson *et al.,* 1994; Kelly, 1999; Wakabayashi and Anusavice, 2000) argue that it is the inner-surface cracks that are most likely to lead to clinical crown failures. Those studies, coupled with finite element modeling, noted empirical dependencies of critical fracture loads on ceramic thickness and ceramic/substrate elastic modulus ratio. However, the explicit form of these dependencies and the role of other material parameters (strength, toughness, hardness) were not determined.

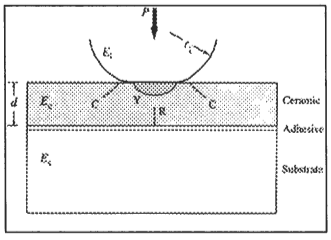

Figure 1. Schematic of brittle layer of thickness d and modulus E_C on a compliant substrate of modulus E_S, depicting sphere indenter of radius r_i. (Specimen radius r_c in general relation Eq. 1a is effectively infinite in the flat layer structure depicted here.) Damage modes: surface cone cracks (C); *quasi*-plastic yield zone (Y); inner-surface flexural radial cracks (R).

Basic Fracture Mechanics Relations

Recently, explicit analytical fracture mechanics relations expressing critical contact loads for each damage mode in terms of basic material and geometrical parameters (elastic modulus, toughness, hardness, strength) and critical geometrical variables (layer thickness, indenter radius) have been developed for bilayer brittle-ceramic/soft-substrate structures (Lawn *et al.*, 2000; Rhee *et al.*, 2001b). Such relations open the way to rational design of ceramic-based crown structures.

Consider the flat-layer system of Fig. 1, consisting of a single ceramic layer of thickness d and Young's modulus E_c bonded onto a compliant thick substrate of modulus E_S, subjected to contact at load P with a sphere of radius r_i and modulus E_i. From the theory of Hertzian elastic contact, it is convenient to generalize the description by defining an "effective sphere radius" r and "effective ceramic modulus" E (Rhee *et al.*, 2001a):

$$1/r = 1/r_c + 1/r_i \qquad (1a)$$

$$1/E = 1/E_c + 1/E_i \qquad (1b)$$

This allows us to account for indenters of different modulus and specimens of different curvature, pertinent to dental structures. For a rigid sphere on flat layer ($E_i \to \infty$, $r_c \to \infty$), $E = E_c$ and $r = r_i$.

Fig. 1 depicts three basic ceramic-layer damage modes, for which the critical load relations are as follows (Lawn *et al.*, 2000; Rhee *et al.*, 2001a,b):

(i) Cone cracks (C)

This kind of fracture initiates from the top surface outside the contact circle, where the Hertzian tensile stress is maximum. The crack first grows downward as a stable, shallow surface ring, resisted by the material toughness T (K_{Ic}), before propagating unstably and arresting in its ultimate cone-like geometry. The critical load for crack pop-in is

$$P_C = A(T^2/E)r \qquad (2)$$

with dimensionless constant $A = 8.6 \times 10^3$ from fits to data from monolithic ceramics with known toughness (Rhee *et al.*, 2001a).

(ii) *Quasi*-plasticity (Y)

Yield initiates when the maximum shear stress in the Hertzian near-field exceeds one-half the yield stress for plastic deformation, which in turn is proportional to the material hardness H (load/projected area, Vickers indentation). The critical load is given by

$$P_Y = DH(H/E)^2 r^2 \qquad (3)$$

with dimensionless constant $D = 0.85$ from fits to data for monolithic ceramics with known hardness (Rhee *et al.*, 2001a).

(iii) Radial cracks (R)

These cracks initiate spontaneously from a starting flaw in the inner ceramic surface when the maximum tensile stress in this surface equals the bulk flexure strength σ_F of the ceramic, at critical load

$$P_R = B\sigma_F d^2/\log(E_c/E_s) \qquad (4)$$

with dimensionless constant $B = 2.0$ from data fits to well-characterized bilayer material systems (Rhee *et al.*, 2001b).

In this paper, we examine the hypothesis that the critical loads for dominant flexural radial cracking vary as the square of layer thickness, as predicted by Eq. 4, at ceramic layer thicknesses less than 1 mm.

MATERIALS & METHODS

Single-cycle Hertzian contact experiments were conducted on crown-like ceramic layers bonded to dentin-like soft support substrates (Rhee *et al.*, 2001b). The ceramic materials used in this study are listed in the Table, along with commercial sources and pertinent properties. Ceramic materials were supplied by the manufacturers in the form of plates with minimum lateral surface dimension of 15 mm. These were ground flat and parallel, and upper and lower ceramic surfaces were polished with 1 μm diamond paste, to thicknesses in the range 100 μm to 6 mm. The ceramic layers were bonded to thick (12.7 mm) transparent polycarbonate support substrates (previous work indicates that increasing substrate layer thicknesses above 2 mm do not strongly influence Hertzian contact damage [Miranda *et al.*, 2001]). Bonding was effected by means of an epoxy adhesive (Harcos Chemicals, Bellesville, NJ, USA) under light pressure for 24 hrs. The resultant thin (10-20 μm) adhesive interlayer was also transparent, with elastic properties similar to those of the polycarbonate base, so that viewing of subsurface radial cracks would not be impaired (Chai *et al.*, 1999; Chai and Lawn, 2000).

Hertzian tests with tungsten carbide spheres of radius r (= r_c) = 3.96 mm mounted into the crosshead of an Instron universal testing machine (Instron Model 1122, Instron, Canton, MA, USA) were conducted on the layer structures. Single load-unload cycles were applied at each contact site at a fixed crosshead speed of 0.15 mm/min, in air.

Radial crack initiation and evolution were monitored *in situ* from below the contact through the transparent adhesive/polycarbonate sublayer by means of an optical zoom microscope with a video tape recorder (Optem, Santa Clara, CA, USA) (Chai *et al.*, 1999; Chai and Lawn, 2000; Kim *et al.*, 2001). (In polycrystalline ceramics, the microstructures provide an abundance of natural flaw sites for radial crack initiation [Lawn, 1993].) The contact load from the testing machine output was recorded on the tape as a picture-in-picture inset. Means and standard deviations for P_R were determined directly from the videotape, for a minimum of n = 5 indentations on each determination. An alternative procedure was used to determine the onset of cone cracking and *quasi*-plasticity in the opaque ceramic layers (Peterson *et al.*, 1998a). Rows of indentations were made on each layer surface at incrementally increasing peak loads, and the indented outer surfaces were gold-coated and examined *a posteriori* in Nomarski illumination. Mean and uncertainty bounds for P_C were determined from the loads over which surface ring cracks first appeared as incipient shallow arcs (lower limit) and were fully formed (upper limit), minimum n = 5. Values for P_Y were similarly determined as the load ranges over which the residual surface impressions were completely undetectable and were clearly visible.

To facilitate data comparisons between any two materials, we made regression analyses on the P_R critical load data as a function of ceramic layer thickness d for each bilayer system, and correlation coefficients were determined.

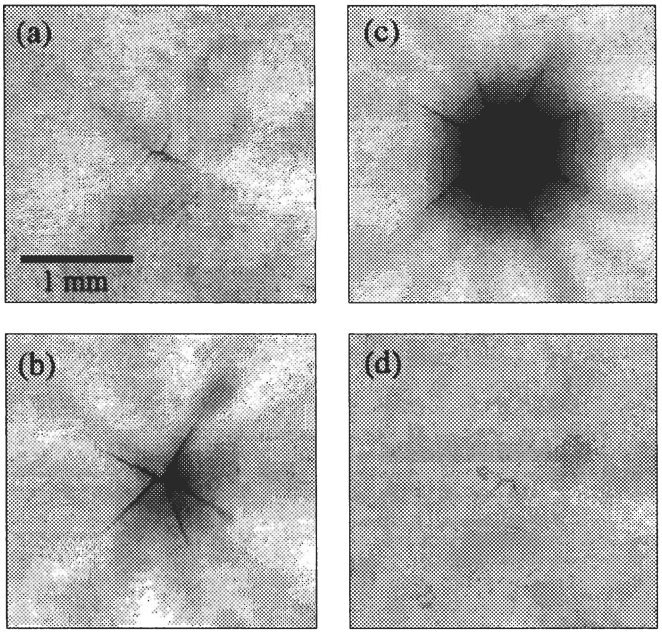

Figure 2. Radial crack sequence in glass-infiltrated alumina layer, thickness d = 155 μm, on polycarbonate substrate, from indentation with WC sphere of radius r = 3.96 mm. Sequence during loading cycle at **(a)** P = 15.1 N (critical), **(b)** P = 35.1 N (intermediate), **(c)** P = 56.6 N (peak), and **(d)** P = 0 N (fully unloaded).

RESULTS

Fig. 2 shows a micrographic sequence of radial crack evolution in one bilayer system, glass-infiltrated-alumina/polycarbonate, video-recorded through the bottom of the transparent substrate during one complete Hertzian loading cycle. The example is for a relatively thin alumina layer, d =155 μm, at a sphere radius r = 3.96 mm, but the observations are quite representative of all thicknesses studied, including those in the clinically relevant region 500 μm to 1.5 mm. The sequence shows how radial cracks initiate (pop-in) at a critical load, multiply, and extend as the indenter load is increased beyond this threshold, and ultimately close up and become almost invisible as the indenter is withdrawn. (Reloading regenerates the same pattern, indicating that the cracks do not heal and therefore remain dangerous.) These cracks have a typically elongate geometry, with lateral dimension ≈ d and through-thickness dimension ≈ 0.5 d at pop-in. At higher loads, the radial cracks became even more elongate, sometimes propagating to the edge of the specimen (full failure). No delamination occurred at the ceramic/polycarbonate interface in our experiments, despite the weak epoxy bond and the metallized alumina undersurface.

Critical loads for the onset of first-observed damage in each of the model ceramic/polycarbonate bilayer systems are shown in Fig. 3a as a function of layer thickness d, at fixed sphere radius r = 3.96 mm. Filled symbols are P_R data for radial cracking, unfilled symbols are P_C data for cone cracking ($P_C < P_Y$) or P_Y data for yield ($P_Y < P_C$). Solid lines are *a priori* predictions from Eqs. 1-4 based on the material parameters in the Table. In the thicker ceramic layers ($d \geq 1$ mm), first damage initiates from the outer, top surface, as cone cracks in the porcelain but as *quasi*-plasticity in the alumina and zirconia. In the thinner layers ($d \leq 1$ mm), radial cracks initiate first. Especially noteworthy in the latter region is the high

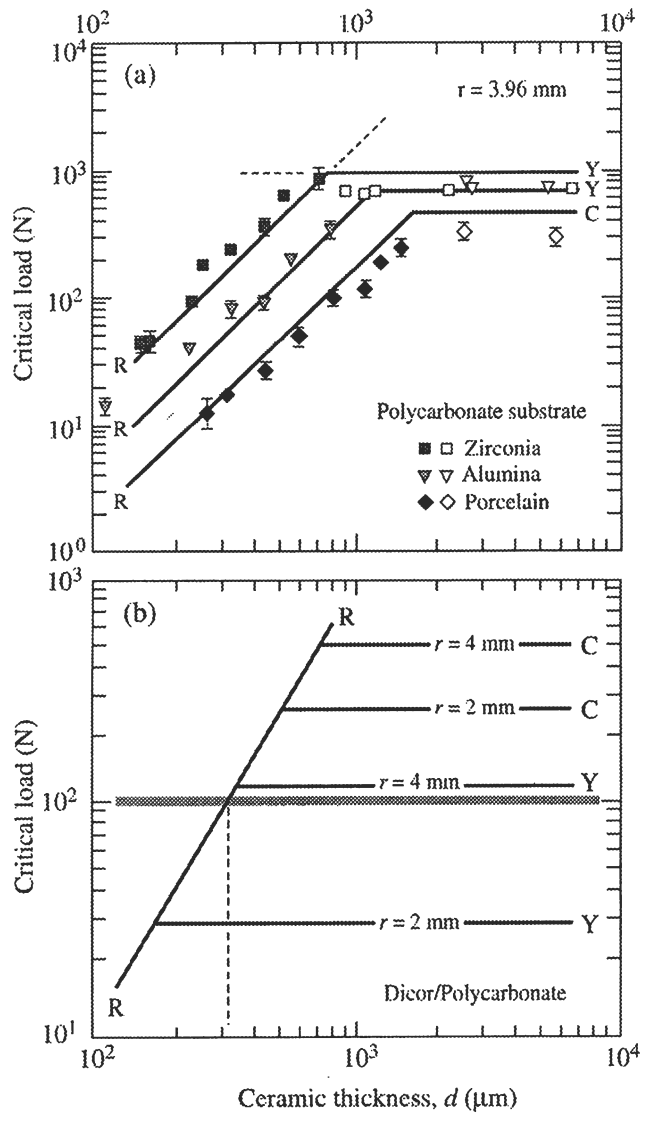

Figure 3. Critical load for first damage as function of layer thickness d, for ceramic/polycarbonate bilayers indented with WC spheres. **(a)** Results for zirconia, alumina, and porcelain specimens, fixed sphere radius r = 3.96 mm. Filled symbols are P_R data (R), unfilled symbols are P_C data (C) or P_Y data (Y). Minimum n = 5 indentations each data point, standard deviation limits shown (some less than the size of the symbol). Solid lines are theoretical first-damage predictions for radial and cone cracking or *quasi*-plasticity. (Regression fits not shown.) **(b)** Predictions from Eq. 4 for hypothetical Dicor/polycarbonate bilayers, sphere radii r = 4 mm and 2 mm. Inclined lines—radial cracking (R); horizontal lines—cone cracking (C) or *quasi*-plasticity (Y). Shaded line represents a nominal occlusal load of 100 N, dashed vertical line indicates the corresponding thickness (≈ 0.3 mm) at which this load will induce flexural radial cracking.

sensitivity of P_R to d, covering more than 2 orders of magnitude over the thickness test range. The relative positions of the P_R (d) data for the 3 materials are commensurate with the strength values in the Table.

Linear regression of log P_R on log d^2 raw data for each material represented in Fig. 3a gave correlation coefficients r = 0.993 (porcelain) and 0.985 (alumina) and 0.980 (zirconia). The theoretical prediction of log P_R on log d^2 from Eq. 4 relative to the data provided errors of estimation $1 - r^2$ = 1.5%

Table. Properties of Dental Materials[a]

Material	Product Name[b]	Supplier	Modulus E (GPa)	Hardness[c] H (GPa)	Toughness T (MPa.m$^{1/2}$)	Strength σ_F (MPa)
Ceramics						
Porcelain	Mark II	Vita Zahnfabrik	68	6.4	0.92	130
Alumina (infiltrated)	In-Ceram	Vita Zahnfabrik	270	12.3	3.0	500
Zirconia (Y-TZP)	Prozyr	Norton	205	12.0	5.4	1450
Glass-ceramic[d]	Dicor	Dentsply	69	3.8	1.1	300
Substrates						
Polycarbonate	Hyzod	AIN Plastics	2.3	0.15	—	—
Dentin	—	Natural	20	0.60	—	—
Indenter						
Tungsten carbide	Kennametal	J & L Industrial	614	19.0	—	—

[a] Data courtesy of I.M. Peterson, Y.-W. Rhee, J. Quinn, and H. Xu (unpublished data). Maximum uncertainties estimated at 5% in E, 10% in H, 15-20% in T, 15-20% in σ_F.
[b] Information on product names and suppliers in this paper is not to imply endorsement by NIST.
[c] Indentation hardness, $H = 2P/d^2 = 1.078\ H_V$, d = indent diagonal.
[d] Included as case study material.

(porcelain), 2.5% (alumina), and 4.8% (zirconia). This analysis validates the hypothesis that the critical loads for flexural radial cracking are explicitly dependent on the square of the layer thickness, and provides a sound physical basis for rating materials performance.

DISCUSSION

Fundamental damage modes in flat dental ceramic layers on soft substrates in contact loading that simulates the basic elements of occlusal function have been confirmed for ceramic crown layers with clinically relevant thicknesses. Critical loads to initiate each mode have been measured for selected dental ceramic materials, as a function of layer thickness and contacting sphere radius. *In situ* observations of the inner ceramic surfaces through the base of the transparent substrate material facilitate determination of critical initiation loads for radial cracks, as well as of subsequent evolution of these cracks to failure. These radial cracks are of primary interest for their clinical relevance (Kelly *et al.*, 1990; Thompson *et al.*, 1994; Tsai *et al.*, 1998)—they can form at relatively low loads in thinner layers and thereafter grow over long distances subsurface. The observations in Fig. 2 suggest that such subsurface radial cracks may be hard to detect in clinical examinations, especially in opaque crowns on dentin substrates. Fig. 3a shows that cone cracking or *quasi*-plasticity becomes the dominant damage mechanism above a certain threshold thickness for each ceramic. Such a shift in damage mechanism may not always be apparent in routine testing, depending on contact conditions—for instance, no such shift to cone cracking was reported in flexure tests on Dicor/epoxy-resin plates (Tsai *et al.*, 1998), where adhesive tape (thickness, 0.6 mm) on the top surface and a relatively blunt (1.6-mm-diameter flatended punch) indenter were deliberately used to reduce the contact stress concentration.

The critical load data in Fig. 3a have been analyzed in terms of analytical fracture mechanics relations (Eqs. 1-4) for each damage mode. Statistical analysis of the flexural radial crack data (correlation coefficients > 0.98) confirms the hypothesis that these relations have the capacity to account for essential data trends. The relations explicitly identify controlling geometric and material parameters. For the outer-surface cone cracking and *quasi*-plasticity modes, it is sphere radius r and toughness T or hardness H that control. For the inner-surface flexural radial crack mode, layer thickness d and strength σ_F are the crucial parameters—modulus mismatch E_c/E_s enters only as a relatively slow logarithmic dependence. In the case of radial cracks, the critical load varies as the square of the ceramic layer thickness, $P_R \propto d^2$.

The fracture mechanics relations thereby facilitates *a priori* predictions of critical loads for ceramic-crown-like bilayer systems. Our experiments have been performed on soft polycarbonate substrates (E_S = 2.35 GPa) for experimental convenience. In real crown systems, the modulus of dentin is substantially higher (E_s =16 GPa) (Xu *et al.*, 1998; Kinney *et al.*, 1999). Recent contact studies for soda-lime glass (E_s = 70 GPa; *cf.* E_s = 68 GPa for porcelain) on a broad range of compliant substrates (E_s = 2.35-44 GPa) have confirmed the logarithmic E_c/E_s dependence in Eq. 4 (Lee *et al.*, 2000). According to Eq. 4, therefore, replacing E_s for polycarbonate with that for dentin will simply shift the $P_R(d)$ curves upward in Fig. 3a. Also in real crown systems, the cuspal radius r_c of the crown is finite (*cf.* $r_c = \infty$ for flat-layer systems). From Eqs. 1-3, decreasing r_c from infinity will shift the $P_C(d)$ and $P_Y(d)$ curves downward in Fig. 3a. As an illustrative case study, consider a monolithic glass-ceramic (Dicor) crown on dentin substrate, in occlusal contact with tooth enamel (E_i = 94 GPa), assuming $r_i = r_c$. Fig. 3b is a design diagram constructed according to Eqs. 1-4, in conjunction with appropriate material parameters from the Table, in analogy to Fig. 3a. Predictions are shown for P_R, P_C, and P_Y at two cuspal radii, r_c = 2 and 4 mm. The horizontal band at P_* = 100 N represents a nominal molar biting force. Minimum conditions to survive dental function are that (i) the ceramic thickness should remain above 1 mm, to avoid radial cracking, and (ii) the cuspal radius should

remain above 4 mm, to avoid *quasi*-plasticity (or cone cracking). While studies of failed Dicor crowns indicate ceramic thicknesses > 1 mm in almost all cases (Malament and Socransky, 1999), the especially high susceptibility of glass ceramics to *quasi*-plasticity (Peterson *et al.*, 1998b) (attributable to a relatively low hardness) may account for the unacceptably high failure rates of Dicor molar crowns in clinical practice (Malament and Socransky, 1999; Sjogren *et al.*, 1999). In harder ceramics, radial cracking is expected to be the dominant mode of failure.

Of interest is the appearance of strength σ_F in Eq. 4 for radial cracking. The strength of ceramics varies with the inverse square root of flaw size (Lawn, 1993). In polycrystalline ceramics, especially those with coarser grain structures, such flaws are generally intrinsic to the microstructure (Peterson *et al.*, 1998b). For ceramics with more refined microstructures, dominant flaws may be introduced in surface handling or preparation, *e.g.*, by sandblasting or grinding ("machining flaws"), or from preparation and manufacturing problems (voids). One should therefore take care to avoid large surface flaws in the undersurface of the brittle layer, to prevent the $P_R(d)$ function from shifting downward in Fig. 3. At the same time, P_C in Eq. 2 and P_Y in Eq. 3 are relatively insensitive to starting flaw size (Langitan and Lawn, 1969).

Some restrictions in our analysis are acknowledged. We have considered only flat-surface ceramic monolayers on soft substrates, with virtually no intervening adhesive layer. Real crowns consist of ceramic veneer/core bilayers, with convoluted cuspal/occlusal geometries and complex loading, bonded to dentin with cement layers that may be 100 μm or more thick and contain voids. Recent work on ceramic veneer/core bilayers indicates that the veneer/core thickness ratio can be a crucial variable in failure mechanics, especially for radial cracking (Wakabayashi and Anusavice, 2000; Miranda *et al.*, 2001). The compliance of even the thinnest adhesives (down to 10 μm) can have disproportionately large effects, especially between two adjoining stiff layers (Chai and Lawn, 2000). Cyclic contact loading of monolithic ceramics has been shown to cause cumulative strength degradation in a variety of dental ceramics (Jung *et al.*, 2000)—others have demonstrated analogous degradation in all-ceramic crowns bonded to dentin-like substrates (Chen *et al.*, 1999). These complicating factors may ultimately be best evaluated in artificial mouth-motion machines. Nevertheless, the procedure outlined here affords a simple route to the materials characterization of layered dental ceramics, and provides a sound physical basis for design against lifetime-threatening damage in simulated occlusal conditions.

ACKNOWLEDGMENTS

Thanks are due to H.-W. Kim, I.M. Peterson, Y.-W Rhee, J. Quinn, and H. Xu at NIST for providing some of the data in the Table. Specimen materials were generously supplied by H. Hornberger of Vita Zahnfabrik, Bad Sackingen, Germany, and E. Levadnuk of Norton Desmarquest Fine Ceramics, East Granby, CT, USA. This study was supported by a grant from the US National Institute of Dental and Craniofacial Research, POI DE10976.

REFERENCES

Chai H, Lawn BR (2000). Role of adhesive interlayer in transverse fracture of brittle layer structures. *J Mater Res* 15:1017-1024.

Chai H, Lawn BR, Wuttiphan S (1999). Fracture modes in brittle coatings with large interlayer modulus mismatch. *J Mater Res* 14:3805-3817.

Chen HY, Hickel R, Setcos JC, Kunzelmann KH (1999). Effects of surface finish and fatigue testing on the fracture strength of cad-cam and pressed-ceramic crowns. *J Prosthet Dent* 82:468-475.

DeLong R, Douglas WE (1983). Development of an artificial oral environment for the testing of dental restoratives: bi-axial force and movement control. *J Dent Res* 62:32-36.

Guiberteau F, Padture NP, Cai H, Lawn BR (1993). Indentation fatigue: a simple cyclic Hertzian test for measuring damage accumulation in polycrystalline ceramics. *Philos Mag* 68(A):1003-1916.

Jung YG, Wuttiphan S, Peterson IM, Lawn BR (1999). Damage modes in dental layer structures. *J Dent Res* 78:887-897.

Jung Y-G, Peterson IM, Kim DK, Lawn BR (2000). Lifetime-limiting strength degradation from contact fatigue in dental ceramics. *J Dent Res* 79:722-731.

Kelly JR (1997). Ceramics in restorative and prosthetic dentistry. *Ann Rev Mater Sci* 27:443-468.

Kelly JR (1999). Clinically relevant approach to failure testing of all-ceramic restorations. *J Prosthet Dent* 81:652-661.

Kelly JR, Giordano R, Pober R, Cima MJ (1990). Fracture surface analysis of dental ceramics: clinically failed restorations. *Int J Prosthodont* 3:430-440.

Kim H-W, Deng Y, Miranda P, Pajares A, Kim DK, Kim H-E, *et al.* (2001). Effect of flaw state on the strength of brittle coatings on soft substrates. *J Am Ceram Soc* 84:2377-2384.

Kinney NH, Balooch M, Marshall GM, Marshall SJ (1999). A micromechanics model of the elastic properties of human dentine. *Arch Oral Biol* 44:813-822.

Langitan FB, Lawn BR (1969). Hertzian fracture experiments on abraded glass surfaces as definitive evidence for an energy balance explanation of Auerbach's law. *J Appl Phys* 40:4009-4017.

Lawn BR (1993). Fracture of brittle solids. Cambridge: Cambridge University Press, Chs. 8,9.

Lawn BR (1998). Indentation of ceramics with spheres: a century after Hertz. *J Am Ceram Soc* 81:1977-1994.

Lawn BR, Lee KS, Chai H, Pajares A, Kim DK, Wuttiphan S, *et al.* (2000). Damage-resistant brittle coatings. *Adv Eng Mater* 2:745-748.

Lee KS, Rhee Y-W, Blackburn DH, Lawn BR, Chai H (2000). Cracking of brittle coatings adhesively bonded to substrates of unlike modulus. *J Mater Res* 15:1653-1656.

Malament KA, Socransky SS (1999). Survival of Dicor glass-ceramic dental restorations over 14 years: I. Survival of Dicor complete coverage restorations and effect of internal surface acid etching, tooth position, gender and age. *J Prosthet Dent* 81:23-32.

Miranda P, Pajares A, Guiberteau F, Cumbrera FL, Lawn BR (2001). Contact fracture of brittle bilayer coatings on soft substrates. *J Mater Res* 16:115-126.

Peterson IM, Pajares A, Lawn BR, Thompson VP, Rekow ED (1998a). Mechanical characterization of dental ceramics using Hertzian contacts. *J Dent Res* 77:589-602.

Peterson IM, Wuttiphan S, Lawn BR, Chyung K (1998b). Role of microstructure on contact damage and strength degradation of micaceous glass-ceramics. *Dent Mater* 14:80-89.

Rhee Y-W, Kim H-W, Deng Y, Lawn BR (2001a). Brittle fracture versus quasiplasticity in ceramics: a simple predictive index. *J Am Ceram Soc* 84:561-565.

Rhee Y-W, Kim H-W, Deng Y, Lawn BR (2001b). Contact-induced damage in ceramic coatings on compliant substrates: fracture mechanics and design. *J Am Ceram Soc* 18:1066-1072.

Scherrer SS, Rijk WGd (1993). The fracture resistance of all-ceramic crowns on supporting structures with different elastic moduli. *Int J Prosthodont* 6:462-467.

Scherrer SS, Rijk WGd, Belser UC, Meyer J-M (1994). Effect of cement film thickness on the fracture resistance of a machinable glass-ceramic. *Dent Mater* 10:172-177.

Sjogren G, Lantto R, Tillberg A (1999). Clinical evaluation of all-ceramic crowns (Dicor) in general practice. *J Prosthet Dent* 81:277-284.

Thompson JY, Anusavice KJ, Naman A, Morris BF (1994). Fracture surface characterization of clinically failed all-ceramic crowns. *J Dent Res* 73:1824-1832.

Tsai Y-L, Petsche PE, Yang MC, Anusavice KJ (1998). Influence of glass-ceramic thickness on Hertzian and bulk fracture mechanisms. *Int J Prosthodont* 11:27-32.

Wakabayashi N, Anusavice KJ (2000). Crack initiation modes in bilayered alumina/porcelain disks as a function of core/veneer thickness ratio and supporting substrate thickness. *J Dent Res* 79:1398-1404.

Wuttiphan S, Lawn BR, Padture NP (1996). Crack suppression in strongly-bonded homogeneous/heterogeneous laminates: a study on glass/glass-ceramic bilayers. *J Am Ceram Soc* 79:634-640.

Xu HHK, Smith DT, Jahanmir S, Romberg E, Kelly JR, Thompson VP (1998). Indentation damage and mechanical properties of human enamel and dentin. *J Dent Res* 77:472-480.